

LETTER TO THE EDITOR

Herschel observations of EXtra-Ordinary Sources (HEXOS): Detection of hydrogen fluoride in absorption towards Orion KL[★]

T. G. Phillips¹, E. A. Bergin², D. C. Lis¹, D. A. Neufeld³, T. A. Bell¹, S. Wang², N. R. Crockett², M. Emprechtinger¹, G. A. Blake¹, E. Caux^{4,5}, C. Ceccarelli⁶, J. Cernicharo⁷, C. Comito⁸, F. Daniel^{7,9}, M.-L. Dubernet^{10,11}, P. Encrenaz⁹, M. Gerin⁹, T. F. Giesen¹², J. R. Goicoechea⁷, P. F. Goldsmith¹³, E. Herbst¹⁴, C. Joblin^{4,5}, D. Johnstone¹⁵, W. D. Langer¹³, W. D. Latter¹⁶, S. D. Lord¹⁶, S. Maret⁶, P. G. Martin¹⁷, G. J. Melnick¹⁸, K. M. Menten⁸, P. Morris¹⁶, H. S. P. Müller¹², J. A. Murphy¹⁹, V. Ossenkopf^{12,20}, J. C. Pearson¹³, M. Pérault⁹, R. Plume²¹, S.-L. Qin¹², P. Schilke^{8,12}, S. Schlemmer¹², J. Stutzki¹², N. Trappe¹⁹, F. F. S. van der Tak²¹, C. Vastel^{4,5}, H. W. Yorke¹³, S. Yu¹³, J. Zmuidzinas¹, A. Boogert¹⁶, R. Güsten⁸, P. Hartogh²², N. Honingh¹², A. Karpov¹, J. Kooi¹, J.-M. Krieg⁹, and R. Schieder¹²

(Affiliations are available in the online edition)

Received 30 March 2010 / Accepted 20 April 2010

ABSTRACT

We report a detection of the fundamental rotational transition of hydrogen fluoride in absorption towards Orion KL using *Herschel*/HIFI. After the removal of contaminating features associated with common molecules (“weeds”), the HF spectrum shows a P-Cygni profile, with weak redshifted emission and strong blue-shifted absorption, associated with the low-velocity molecular outflow. We derive an estimate of $2.9 \times 10^{13} \text{ cm}^{-2}$ for the HF column density responsible for the broad absorption component. Using our best estimate of the H₂ column density within the low-velocity molecular outflow, we obtain a lower limit of $\sim 1.6 \times 10^{-10}$ for the HF abundance relative to hydrogen nuclei, corresponding to $\sim 0.6\%$ of the solar abundance of fluorine. This value is close to that inferred from previous ISO observations of HF $J = 2-1$ absorption towards Sgr B2, but is in sharp contrast to the lower limit of 6×10^{-9} derived by Neufeld et al. for cold, foreground clouds on the line of sight towards G10.6-0.4.

Key words. ISM: abundances – ISM: molecules – submillimeter: ISM

1. Introduction

Hydrogen fluoride (HF) is expected to be the main reservoir of fluorine in the interstellar medium because it is easily produced by the exothermic reaction of F with H₂ (Neufeld et al. 2005; Neufeld & Wolfire 2009) and its very strong chemical bond makes this molecule relatively insensitive to UV photodissociation. Interstellar HF was first detected by Neufeld et al. (1997) with ISO. The $J = 2-1$ rotational transition was observed in absorption towards Sgr B2, at a low spectral resolution using the ISO long-wavelength spectrometer (LWS). The HIFI instrument (de Graauw et al. 2010) aboard the *Herschel* Space Observatory (Pilbratt et al. 2010) has allowed observations of the ground state rotational transition of HF at 1.232 THz to be performed for the first time, at high spectral resolution. This transition is expected to be generally observed in absorption because of the very large A coefficient (e.g. Neufeld et al. 2010). Only extremely dense regions could possibly generate enough collisional excitation to yield an HF feature with a positive frequency-integrated flux.

A full HIFI spectral scan of band 5a, with frequency coverage from 1.109 to 1.239 THz, was carried out as part of the guaranteed time key program *Herschel observations of EXtra-Ordinary Sources: The Orion and Sagittarius B2*

star-forming regions (HEXOS). With a strong continuum, it might be expected that Orion would exhibit numerous absorption lines; however it is well known to exhibit no absorption lines at mm wavelengths. For instance even CO $J = 1-0$, which is seen with self-reversals towards many star-forming regions, has a smooth emission line profile with no self-absorption (e.g. Tauber et al. 1991). The lack of absorption has been attributed to competing excitation gradients (external heating from θ^1C and internal heating from the embedded massive protostars), the location of the HII region on the front of the cloud, and the presence of numerous unresolved dense ($n_{\text{H}_2} > 10^5 \text{ cm}^{-3}$) clumps along the line of sight (Tauber et al. 1991). At shorter wavelengths some evidence for absorption is found. Betz & Boreiko (1989) find that the blue side of the fundamental rotational transition of OH is completely absorbed, with only a redshifted emission component. The far-infrared survey of Lerate et al. (2006) with ISO-LWS (188 to 44 μm), has shown that the shapes of water and OH lines gradually change from pure emission at the longest wavelengths to mostly P-Cygni profiles at the shortest wavelengths. At even shorter mid-infrared wavelengths, strong water absorption has been detected by Wright et al. (2000) using ISO-SWS. With the $\sim 10 \text{ km s}^{-1}$ resolution of the SWS Fabry Perot, the absorption is shown to be blue-shifted with respect to the source systemic velocity, extending down to about -50 km s^{-1} . In recent observations with the CRIRES spectrograph on the Very Large Telescope, Beuther et al. (2010)

[★] *Herschel* is an ESA space observatory with science instruments provided by European-led Principal Investigator consortia and with important participation from NASA.

have obtained spectra of the R-branch of the $v = 1-0$ band of both ^{13}CO and ^{12}CO toward the BN object and “source n” within Orion KL. These spectra, which are consistent with earlier spectra obtained at lower resolution and signal-to-noise ratio by Scoville et al. (1983), also show strong absorption at velocities between about -25 and 12 km s^{-1} . As we will discuss below, the particular excitation of these lines (ground rotational state HF and ground vibrational state CO) makes them strong candidates to be seen in absorption, provided favorable geometry and strong background continuum exist. Ground state rotational lines of water isotopologues have similar excitation requirements and HIFI observations of para- H_2^{18}O and para- H_2^{17}O , observed separately in band 4b, are also discussed here.

2. Observations

HIFI observations presented here were carried out on March 6, 2010 using the dual beam switch (DBS) mode pointed towards the Orion Hot Core at $\alpha_{J2000} = 5^{\text{h}}35^{\text{m}}14.3^{\text{s}}$ and $\delta_{J2000} = -5^{\circ}22'36.7''$. The DBS reference beams lie approximately $3'$ east and west (i.e. perpendicular to the orientation of the Orion Molecular Ridge; e.g. Ungerechts et al. 1997). We used the Wide Band Spectrometer providing a spectral resolution of 1.1 MHz (0.26 km s^{-1}) over a 4 GHz IF bandwidth. Although both H and V polarization data were obtained, we only present here data from the H polarization, reduced using HIPE (Ott 2010) with pipeline version 2.4.

The band 4b and 5a spectral scans consist of double sideband spectra with a redundancy of 6, which gives observations of a lower or upper sideband frequency with 6 different frequency settings of the local oscillator. This allows for the deconvolution and isolation of a single sideband spectrum (Comito & Schilke 2002). We applied the standard HIFI deconvolution using the *doDeconvolution* task within HIPE. All data presented here are deconvolved single sideband spectra, including the continuum. Regions of the spectrum free of lines were isolated and give a typical rms of $T_A^* = 0.17 \text{ K}$ at the original spectral resolution. The HIFI beam size at 1.23 THz is $17''$, with an assumed main beam efficiency of 0.67.

A $^{13}\text{CO } J = 2-1$ spectrum towards Orion BN/KL was also obtained using the facility receiver and spectrometers of the Caltech Submillimeter Observatory (CSO) atop Mauna Kea in Hawaii. The CSO beam size at 220 GHz is $\sim 33''$ and the main beam efficiency is ~ 0.68 .

3. Results

3.1. First detection of submm absorption towards Orion

Figure 1 shows the detection of HF $J = 1-0$ and para- $\text{H}_2^{18}\text{O } 1_{11}-0_{00}$ in emission and absorption towards Orion BN/KL (blue and red histograms, respectively). Both lines show high-velocity emission line wings on the red side of the systemic velocity of 9 km s^{-1} , a sharp drop near the systemic velocity, and broad absorption extending towards lower (blue) velocities. In contrast, $^{13}\text{CO } J = 2-1$ emission (black histogram) shows broad line wings superposed on a narrow feature at 9 km s^{-1} , but no evidence for absorption.

There are a number of issues which must be addressed. First these data were obtained using DBS which places the reference beams $3'$ away from the central hot core. This is large enough to avoid any reference position contamination from the hot core and shock, but might encompass emission from the extended molecular ridge. Both HF and para- H_2^{18}O have high dipole moments and fast ($>10^{-2} \text{ s}^{-1}$) spontaneous de-excitation

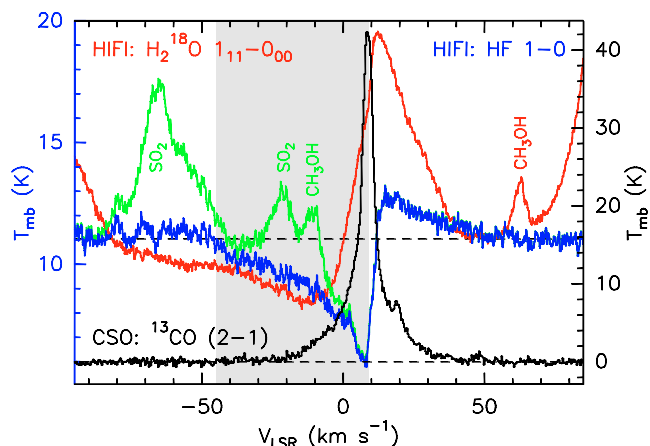


Fig. 1. HIFI detection of interstellar HF $J = 1-0$ (rest frequency 1232.47627 GHz ; Nolt et al. 1987) and para- $\text{H}_2^{18}\text{O } 1_{11}-0_{00}$ (at 1101.698256 GHz) towards Orion BN/KL (blue and red, respectively). The region of low-velocity HF absorption is highlighted in grey. Both observations are from HIFI band 5a and are referenced to the temperature scale on the left. CSO $^{13}\text{CO } J = 2-1$ spectrum towards the same position is shown in black, using the temperature scale on the right. The HF absorption is blended with the emission of CH_3OH ($\sim -10 \text{ km s}^{-1}$) and SO_2 (~ -20 and -65 km s^{-1}), shown in green. Subtraction of these contaminating lines results in the dark blue HF spectrum.

rates leading to critical densities in excess of 10^8 cm^{-3} (Reese et al. 2005; Grosjean et al. 2003). Beyond the hot core, the density is well below this value (Bergin et al. 1996) and, for HF, extended emission is unlikely. This may not be the case for para- H_2^{18}O , as the ground state emission of *ortho*- H_2O is strong and extended (Snell et al. 2000; Olofsson et al. 2003). Because the DBS mode alternates between two reference positions, we have used the Level 1 data to compute a difference spectrum between the two reference positions; we see no evidence for emission or absorption in such a difference spectrum for either line. It is very unlikely that the same level of emission or absorption would be present in the two reference beams, separated by $6'$ on the sky. In addition, the extended emission component in Orion is centered at 9 km s^{-1} and has a narrow line width of $2-5 \text{ km s}^{-1}$. For HF we do see absorption at the systemic velocity, but also a broad blue-shifted absorption. We thus conclude that the observed absorption is real, and not an artifact of the observing mode employed.

3.2. Contamination by interfering lines

In the case of HF there is an additional complication in that the low-velocity blue absorption is blended with emission from $\text{CH}_3\text{OH } J = 21_1-20_0 \text{ E}$ and $\text{SO}_2 J = 30_{7,23}-29_{6,24}$ (see grey area in Fig. 1). A more extensive look at the spectrum near HF $J = 1-0$ is provided in Fig. 2. In this 7 GHz wide region of the spectrum we see multiple prominent lines of both CH_3OH and SO_2 . For CH_3OH , one of the detected transitions is $J = 21_1-20_0 \text{ A}^+$, which has a similar ground state energy and 120% stronger line strength than the $J = 21_1-20_0 \text{ E}$ transition. Thus we confirm the CH_3OH contamination. We have modeled the extensive emission from SO_2 (and CH_3OH) seen in Band 5a assuming LTE (with a correction for optical depth). This analysis also confirms that $\text{SO}_2 J = 30_{7,23}-29_{6,24}$ will emit at appreciable levels and interfere with the HF absorption.

Line contamination by abundant “weed” molecules, such as methanol or SO_2 , will be a common problem affecting HIFI

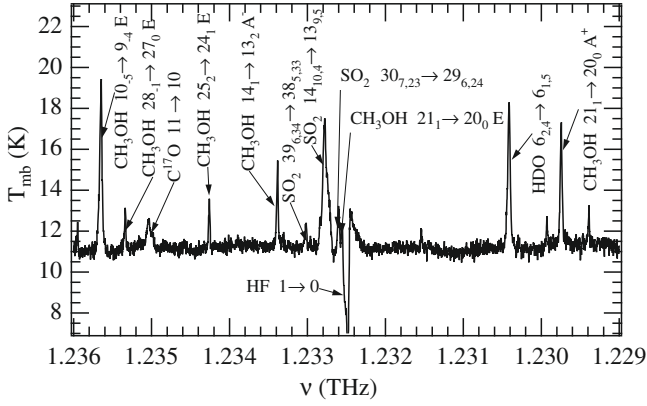


Fig. 2. A more extensive look at the molecular spectrum surrounding HF $J = 1-0$. Transitions of CH₃OH and SO₂ were isolated using the frequencies taken from Müller & Brünken (2005) and Xu et al. (2008). Three lines are blended with (or provide background to) the HF absorption.

observations of molecular hot core sources and modeling tools are being developed to deal with this problem. The two SO₂ lines in the spectrum have been removed using such a model¹. In the case of CH₃OH, the LTE model is not accurate enough to deal with the problem and we removed the interfering line by fitting a single-component gaussian and subtracting the emission. The emission fit and the final HF absorption spectrum are shown in Fig. 3. This spectrum is then used for the analysis in Sect. 4. The HF absorption full-width at zero intensity (FWZI) is $\sim 50 \text{ km s}^{-1}$, which is less than that of para-H₂¹⁸O (FWZI $\sim 80 \text{ km s}^{-1}$). For completeness, in the computation of the line-to-continuum ratio, we also explored the possibility that the CH₃OH and SO₂ lines contribute to the background emission for the absorbing HF gas. This will be reflected in our error analysis.

The analysis is simpler for H₂¹⁸O, which shows no evidence for any contamination within the absorption velocity range. For this line we have assumed a continuum value based on the level measured at frequencies adjacent to the water line.

4. Discussion

After the removal of features attributed to CH₃OH and SO₂, the HF $J = 1-0$ spectrum shows a P-Cygni profile with a broad, blueshifted absorption at LSR velocities between about -45 and 9 km s^{-1} and a redshifted emission component at LSR velocities in the range 12 to 50 km s^{-1} . The analysis of the HF emission, along with other spectral lines detected in Orion, will be discussed in a future paper. The HF spectrum is strikingly similar to that of another transition with an extremely high critical density: the CO fundamental vibrational band (Beuther et al. 2010) which shows the same combination of absorption at LSR velocities between about -25 and 12 km s^{-1} and weak emission extending to $V_{\text{LSR}} \sim 30 \text{ km s}^{-1}$. We suggest that exactly the same physical processes give rise to the CO $v = 1-0$ and HF $J = 1-0$ spectra: outflowing material surrounding the hot core in Orion absorbs and re-emits continuum radiation from the central source. The absorption – occurring in front of the source – naturally gives rise to a blueshifted absorption feature, while re-emission from

¹ We made use of the myXCLASS program (<http://www.astro.uni-koeln.de/projects/schilke/XCLASS>), which accesses the CDMS (Müller et al. 2001, 2005; <http://www.cdms.de>) and JPL (Pickett et al. 1998; <http://spec.jpl.nasa.gov>) molecular data bases.

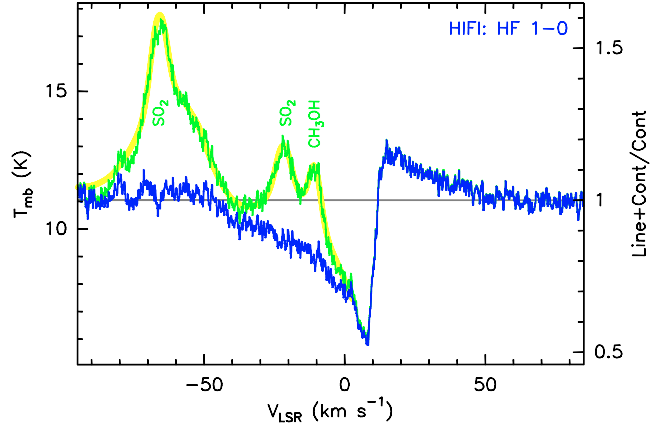


Fig. 3. HIFI HF $J = 1-0$ spectrum (blue-green histogram) with fit to CH₃OH and SO₂ emission shown in yellow. Subtraction of these contaminating lines provides a more complete look at the HF absorption (blue histogram).

the back side of the outflow provides the weak redshifted emission feature. For transitions with a very high critical density, the absorption of a “resonance line photon” (such as HF $J = 1-0$) will inevitably be followed by re-emission. Were the continuum source surrounded by a spherical shell that is small compared to the telescope beam, the areas of the emission and absorption features would be equal. The simplest interpretation of the observed HF $J = 1-0$ spectrum – which shows an absorption feature that is stronger than the emission feature – is that the outflowing material is not entirely encompassed by the beam so that part of the emission flux is unobserved; this explanation could be tested by means of mapping observations.

Most of the material appears to have an outflow velocity $\leq 20 \text{ km s}^{-1}$ and is likely associated with the “Low Velocity Flow” (e.g. Genzel & Stutzki 1989). The para-H₂¹⁸O and para-H₂¹⁷O $1_{11}-0_{00}$ (not shown) lines also show absorption at negative LSR velocities, although the absorption extends further, to LSR velocities as negative as $\sim -80 \text{ km s}^{-1}$. This behavior may reflect the presence of enhanced water abundances in the High Velocity Flow (Franklin et al. 2008). The para-H₂¹⁸O (and para-H₂¹⁷O $1_{11}-0_{00}$) line profiles are also different from HF in exhibiting an emission feature that is stronger than the absorption feature. This behavior must imply that collisional excitation provides an additional excitation mechanism, and may suggest that the rate coefficients for excitation of the para-water transition are significantly larger than those for excitation of the HF transition. To date, the collisional excitation of HF has been computed only in the case where He is the collision partner (Reese et al. 2005); the rate coefficients thereby derived are indeed an order of magnitude smaller than those computed for the excitation of para-water by H₂ (Grosjean et al. 2003), but the rate coefficients for excitation of HF by H₂ might be expected to be larger than those for excitation by He.

We have determined the column density of absorbing molecules responsible for the broad blueshifted absorption features. If the absorbing material is assumed to cover the continuum source, we estimate the velocity-integrated optical depth HF $J = 1-0$ as 11.8 km s^{-1} , which implies an HF column density of $2.9 \times 10^{13} \text{ cm}^{-2}$ if all molecules are in the ground-state. Uncertainties introduced by the need to correct for the SO₂ and CH₃OH emission features result in possible errors that we estimate as about $\pm 25\%$. Derived under the same set of assumptions, the column densities of absorbing para-H₂¹⁸O and para-H₂¹⁷O are $1.3 \times 10^{13} \text{ cm}^{-2}$ and $7 \times 10^{12} \text{ cm}^{-2}$, respectively. Strictly,

these values are all lower limits, because the source could be partially-covered by clumps of arbitrarily large optical depth and the strong continuum could lead to some excitation. In addition, the water lines have strong emission which might lie behind the absorbing material. However, the fact that all three spectral lines show absorption profiles of similar shapes but different depths, suggests that the optical depths are not extremely large.

In order to estimate the molecular abundances implied by these column densities, we require an estimate of the total column density of H_2 . Beuther et al. (2010) used the observed strength of the $^{13}\text{CO } v = 1-0$ absorption features along the sight-line to the BN object, together with standard assumptions about the $^{13}\text{CO}/^{12}\text{CO}$ and CO/H_2 abundance ratios, to derive an H_2 column density of $4.9 \times 10^{22} \text{ cm}^{-2}$ for the outflowing absorbing gas. An alternative estimate has been obtained by Persson et al. (2007) from observations of emission from C^{17}O pure rotational lines; this yields a value $3 \times 10^{23} \text{ cm}^{-2}$ for the total H_2 column density within the Low Velocity Flow, half of which ($1.5 \times 10^{23} \text{ cm}^{-2}$) would be associated with the blue outflow lobe. We have estimated the H_2 column density independently from the strength of the broad $^{13}\text{CO } 2-1$ emission component. Assuming LVG, 100 K kinetic temperature, an H_2 density of $1 \times 10^5 \text{ cm}^{-3}$ (Persson et al. 2007), and a ^{13}CO fractional abundance of 2×10^{-6} (Dickman 1987), we derive $N(\text{H}_2) = 9 \times 10^{22} \text{ cm}^{-2}$ in the blue outflow lobe. This value, intermediate between the Persson et al. and Beuther et al. estimates, is used in the subsequent calculations (a factor of 2 estimated uncertainty).

With these assumptions, our observations of the blueshifted absorption feature imply an HF abundance of 1.6×10^{-10} relative to hydrogen nuclei, corresponding to $\sim 0.6\%$ of the solar abundance of fluorine (Asplund et al. 2009). This value is in sharp contrast with the lower limit $N(\text{HF})/N_{\text{H}} \geq 6 \times 10^{-9}$ obtained by Neufeld et al. (2010) for foreground material along the sight-line to G10.6-0.4, but close to that inferred ($N(\text{HF})/N_{\text{H}} = 1.5 \times 10^{-10}$) from previous observations of HF $J = 2-1$ absorption toward Sgr B2 (Neufeld et al. 1997). Since the density in the Low Velocity Flow, $n(\text{H}_2) \sim 10^5 \text{ cm}^{-3}$ (Persson et al. 2007) is two orders of magnitude larger than the typical density of the foreground material probed in observations of G10.6-0.4, and since HF is expected to be the dominant reservoir of fluorine in the gas-phase, this abundance difference reflects a density-dependent depletion of fluorine nuclei onto grain mantles. A depletion factor $\sim 10^2$ does not seem unreasonable, in light of the polar nature of the HF molecule; indeed, the freezing and boiling points of HF are relatively large (190 K and 293 K respectively at 1 atm. pressure), so – as in the case of interstellar water – the freeze-out of HF can be expected to be quite efficient. On the other hand, shocks of velocity greater than $\sim 15 \text{ km s}^{-1}$ are predicted to release grain mantles into the gas phase as the result of sputtering (Draine 1995). If high depletions are indeed attained in gas traveling at outflow velocities up to $\sim 35 \text{ km s}^{-1}$, then our observations suggest that the acceleration to a given terminal velocity can occur without the material suffering shocks of equal velocity.

5. Conclusions

Our observations of hydrogen fluoride toward Orion-KL have revealed an unusual absorption feature in the spectrum of this source. To our knowledge, this is the first report of a submillimeter spectral line with a net negative flux in this archetypical

emission line source. The unusual behavior of the HF $J = 1-0$ transition is a consequence of its extremely large critical density, and is mirrored by mid-infrared observations of the CO $v = 1-0$ band. Thanks to the high spectral resolution achievable with HIFI, the HF $J = 1-0$ line promises to provide a unique probe of the kinematics of – and depletion within – absorbing material along the sight-line to bright continuum sources, and one that is uncomplicated by the collisionally-excited line emission that is usually present in the spectra of other transitions. Redshifted HF $J = 1-0$ absorption may also prove to be an excellent tracer of the interstellar medium in the high-redshift Universe; the range of redshifts accessible from ground-based submillimeter telescopes is indicated by Neufeld et al. (2005, see their Fig. 11).

Acknowledgements. HIFI has been designed and built by a consortium of institutes and university departments from across Europe, Canada and the United States under the leadership of SRON Netherlands Institute for Space Research, Groningen, The Netherlands and with major contributions from Germany, France and the US. Consortium members are: Canada: CSA, U. Waterloo; France: CESR, LAB, LERMA, IRAM; Germany: KOSMA, MPIfR, MPS; Ireland, NUI Maynooth; Italy: ASI, IFSI-INAF, Osservatorio Astrofisico di Arcetri- INAF; Netherlands: SRON, TUD; Poland: CAMK, CBK; Spain: Observatorio Astronómico Nacional (IGN), Centro de Astrobiología (CSIC-INTA). Sweden: Chalmers University of Technology – MC2, RSS & GARD; Onsala Space Observatory; Swedish National Space Board, Stockholm University – Stockholm Observatory; Switzerland: ETH Zurich, FHNW; USA: Caltech, JPL, NHSC. Support for this work was provided by NASA through an award issued by JPL/Caltech. CSO is supported by the NSF, award AST-0540882.

References

- Asplund, M., Grevesse, N., Sauval, A. J., & Scott, P. 2009, *ARA&A*, 47, 481
 Bergin, E. A., Snell, R. L., & Goldsmith, P. F. 1996, *ApJ*, 460, 343
 Betz, A. L., & Boreiko, R. T. 1989, *ApJ*, 346, L101
 Beuther, H., Linz, H., Bik, A., Goto, M., & Henning, T. 2010, *A&A*, 512, A29
 Comito, C., & Schilke, P. 2002, *A&A*, 395, 357
 de Graauw, Th., et al. 2010, *A&A*, 518, L6
 Dickman, R. L. 1978, *ApJS*, 37, 407
 Draine, B. T. 1995, *Ap&SS*, 233, 111
 Franklin, J., Snell, R. L., Kaufman, M. J., et al. 2008, *ApJ*, 674, 1015
 Genzel, R., & Stutzki, J. 1989, *ARA&A*, 27, 41
 Grosjean, A., Dubernet, M.-L., & Ceccarelli, C. 2003, *A&A*, 408, 1197
 Lerate, M. R., Barlow, M. J., Swinyard, B. M., et al. 2006, *MNRAS*, 370, 597
 Müller, H. S. P., & Brünken, S. 2005, *J. Mol. Spectrosc.*, 232, 213
 Müller, H. S. P., Thorwirth, S., Roth, D. A., & Winnewisser, G. 2001, *A&A*, 370, L49
 Müller, H. S. P., Schlöder, F., Stutzki, J., & Winnewisser, G. 2005, *J. Mol. Struct.*, 742, 215
 Neufeld, D. A., & Wolfire, M. G. 2009, *ApJ*, 706, 1594
 Neufeld, D. A., Zmuidzinas, J., Schilke, P., & Phillips, T. G. 1997, *ApJ*, 488, L141
 Neufeld, D. A., Wolfire, M. G., & Schilke, P. 2005, *ApJ*, 628, 260
 Neufeld, D. A., et al. 2010, *A&A*, 518, L108
 Nolt, I. G., Radostitz, J. V., Dilonardo, G., et al. 1987, *J. Mol. Spectrosc.*, 125, 274
 Olofsson, A. O. H., Olofsson, G., Hjalmarsen, Å., et al. 2003, *A&A*, 402, L47
 Ott, S. 2010, in *Astronomical Data Analysis Software and Systems XIX*, ed. Y. Mizumoto, K.-I. Morita, & M. Ohishi, ASP Conf. Ser., in press
 Persson, C. M., Olofsson, A. O. H., Koning, N., et al. 2007, *A&A*, 476, 807
 Pickett, H. M., Poynter, R. L., Cohen, E. A., et al. 1998, *J. Quant. Spectrosc. Radiat. Transfer*, 60, 883
 Pilbratt, G. L., et al. 2010, *A&A*, 518, L1
 Reese, C., Stoecklin, T., Voronin, A., & Rayez, J. C. 2005, *A&A*, 430, 1139
 Scoville, N., Kleinmann, S. G., Hall, D. N. B., & Ridgway, S. T. 1983, *ApJ*, 275, 201
 Snell, R. L., Howe, J. E., Ashby, M. L. N., et al. 2000, *ApJ*, 539, L93
 Tauber, J. A., Goldsmith, P. F., & Dickman, R. L. 1991, *ApJ*, 375, 635
 Ungerechts, H., Bergin, E. A., Goldsmith, P. F., et al. 1997, *ApJ*, 482, 245
 Wright, C. M., van Dishoeck, E. F., Black, J. H., et al. 2000, *A&A*, 358, 689
 Xu, L.-H., Fisher, J., Lees, R. M., et al. 2008, *J. Mol. Spectrosc.*, 251, 305

-
- ¹ California Institute of Technology, Cahill Center for Astronomy and Astrophysics 301-17, Pasadena, CA 91125, USA
e-mail: tgp@submm.caltech.edu
- ² Department of Astronomy, University of Michigan, 500 Church Street, Ann Arbor, MI 48109, USA
- ³ Department of Physics and Astronomy, Johns Hopkins University, 3400 North Charles Street, Baltimore, MD 21218, USA
- ⁴ Centre d'étude Spatiale des Rayonnements, Université de Toulouse [UPS], 31062 Toulouse Cedex 9, France
- ⁵ CNRS/INSU, UMR 5187, 9 avenue du Colonel Roche, 31028 Toulouse Cedex 4, France
- ⁶ Laboratoire d'Astrophysique de l'Observatoire de Grenoble, BP 53, 38041 Grenoble, Cedex 9, France
- ⁷ Centro de Astrobiología (CSIC/INTA), Laboratorio de Astrofísica Molecular, Ctra. de Torrejón a Ajalvir, km 4 28850, Torrejón de Ardoz, Madrid, Spain
- ⁸ Max-Planck-Institut für Radioastronomie, Auf dem Hügel 69, 53121 Bonn, Germany
- ⁹ LERMA, CNRS UMR8112, Observatoire de Paris and École Normale Supérieure, 24 Rue Lhomond, 75231 Paris Cedex 05, France
- ¹⁰ LPMMA, UMR7092, Université Pierre et Marie Curie, Paris, France
- ¹¹ LUTH, UMR8102, Observatoire de Paris, Meudon, France
- ¹² I. Physikalisches Institut, Universität zu Köln, Zùlpicher Str. 77, 50937 Köln, Germany
- ¹³ Jet Propulsion Laboratory, Caltech, Pasadena, CA 91109, USA
- ¹⁴ Departments of Physics, Astronomy and Chemistry, Ohio State University, Columbus, OH 43210, USA
- ¹⁵ National Research Council Canada, Herzberg Institute of Astrophysics, 5071 West Saanich Road, Victoria, BC V9E 2E7, Canada
- ¹⁶ Infrared Processing and Analysis Center, California Institute of Technology, MS 100-22, Pasadena, CA 91125, USA
- ¹⁷ Canadian Institute for Theoretical Astrophysics, University of Toronto, 60 St George St, Toronto, ON M5S 3H8, Canada
- ¹⁸ Harvard-Smithsonian Center for Astrophysics, 60 Garden Street, Cambridge MA 02138, USA
- ¹⁹ National University of Ireland Maynooth, Ireland
- ²⁰ SRON Netherlands Institute for Space Research, PO Box 800, 9700 AV, Groningen, The Netherlands
- ²¹ Department of Physics and Astronomy, University of Calgary, 2500 University Drive NW, Calgary, AB T2N 1N4, Canada
- ²² MPI für Sonnensystemforschung, 37191 Katlenburg-Lindau, Germany